

Observation of non-contact Casimir friction

Zhujing Xu,¹ Peng Ju,¹ Kunhong Shen,¹ Yuanbin Jin,¹ Zubin Jacob,^{2,3} and Tongcang Li^{1,2,3,4,*}

¹*Department of Physics and Astronomy, Purdue University, West Lafayette, Indiana 47907, USA*

²*Elmore Family School of Electrical and Computer Engineering,
Purdue University, West Lafayette, Indiana 47907, USA*

³*Birck Nanotechnology Center, Purdue University, West Lafayette, Indiana 47907, USA*

⁴*Purdue Quantum Science and Engineering Institute, Purdue University, West Lafayette, Indiana 47907, USA*

(Dated: March 12, 2024)

Quantum mechanics predicts the occurrence of random electromagnetic field fluctuations, or virtual photons, in vacuum. The exchange of virtual photons between two bodies in relative motion could lead to non-contact quantum vacuum friction or Casimir friction. Despite its theoretical significance, the non-contact Casimir frictional force has not been observed and its theoretical predictions have varied widely. In this work, we report the first measurement of the non-contact Casimir frictional force between two moving bodies. By employing two mechanical oscillators with resonant frequencies far lower than those in Lorentz models of electrons in dielectric materials, we have amplified the Casimir frictional force at low relative velocities by several orders of magnitude. We directly measure the non-contact Casimir frictional force between the two oscillators and show its linear dependence on velocity, proving the dissipative nature of Casimir friction. This advancement marks a pivotal contribution to the field of dissipative quantum electrodynamics and enhances our understanding of friction at the nanoscale.

The quantum vacuum friction or Casimir friction has been theoretically studied for more than 40 years [1–7]. After some debates over its existence [8–10], it is now theoretically believed that two non-contact neutral bodies with a relative motion in vacuum will experience a small dissipative force due to quantum vacuum fluctuations that tend to slow down the relative motion. Although many different schemes have been proposed to detect the non-contact Casimir friction [11–21], it has not been observed so far due to experimental challenges [1, 22–24]. Partly due to the lack of experimental results, theoretical predictions of the Casimir friction exhibit considerable variation [2, 25]. In this work, we report the first measurement of the non-contact Casimir frictional force between two moving objects. Our work is not only important in dissipative quantum electrodynamics, but will also benefit the understanding of friction at the nanoscale [26, 27].

Casimir friction between two surfaces arises due to the interaction between instantaneous charges and electrical dipoles on surfaces induced by quantum fluctuations [6]. The dissipation essentially comes from the Doppler shift of the electromagnetic waves reflected by two moving surfaces and the energy eventually dissipates as radiation or heat [6]. To detect such small Casimir friction, several studies have proposed to enhance it by resonant photon tunneling [28–33]. In this case, the mechanical energy of the moving body can be converted to the electromagnetic energy, leading to an evanescent wave resonance. The resonance requires a critical velocity V_0 such that $V_0 = \frac{2\omega_s d}{|n| R_p(\omega_s)}$ [29], where d is the separation between two surfaces, $R_p(\omega) = \frac{\epsilon(\omega)-1}{\epsilon(\omega)+1}$ is the reflection coefficient for p-polarized waves, $\epsilon(\omega)$ is the dielectric function of the material, and ω_s is the surface wave resonance frequency such that $Re(\epsilon(\omega_s)) = -1$. However, this critical velocity is extremely high for conventional dielectric materials and makes the measurement extremely difficult. For a typical dielectric material such as silicon carbide (SiC), the surface wave resonance fre-

quency is $\omega_s = 1.76 \times 10^{14}$ rad/s [34]. At a separation of 100 nm, the resonant velocity is 1.31×10^7 m/s. Such an extremely high required velocity suppresses the possibility of measuring the Casimir friction with a conventional material.

If we can decrease the surface wave resonance frequency, we can greatly reduce the challenge of detecting the non-contact Casimir frictional force. To demonstrate this, we show the calculation of Casimir friction (F_{CF}) due to quantum vacuum fluctuations for different dielectric materials in Fig.1(a), where one solid plate is moving with a velocity v while the other solid plate is stationary[35]. The friction force originates from the interaction between the incident virtual photons (quantum vacuum fluctuations) and the electrons in solids (Fig.1(a)). For simplicity, here we assume two separated plates in relative parallel motion are made of identical materials [28]. The Casimir friction depends on the material properties, the separation between two plates and the relative velocity. The material properties can be described by the dielectric functions and the dielectric functions of plates are modeled by Lorentz models, which treat each discrete vibrational mode as a classical damped harmonic oscillator as shown in Fig.1(b). More details are included in the Supplementary Material Section II. In this case, the energy dissipates through the phonon loss of the vibrational modes in solids.

Figure 1(e) shows the calculation results for SiC [34], barium strontium titanate (BST) [31] and a hypothetical metamaterial. The metamaterial is assumed to have a Lorentz oscillator resonant frequency of $2\pi \times 5$ kHz and a damping rate of $2\pi \times 100$ Hz. The surface wave resonance frequencies are $2\pi \times 2.80 \times 10^{13}$ Hz, $2\pi \times 1.84 \times 10^9$ Hz, $2\pi \times 1.18 \times 10^4$ Hz for SiC, BST and the metamaterial, respectively. Therefore, the critical velocities for resonant photon tunneling at a separation of 100 nm are around 1.3×10^7 m/s, 840 m/s and 5.2×10^{-3} m/s, respectively. In Fig.1(e), we show that the resonant velocity for the metamaterial is more than nine orders lower than the resonant velocity of SiC. This leads to an

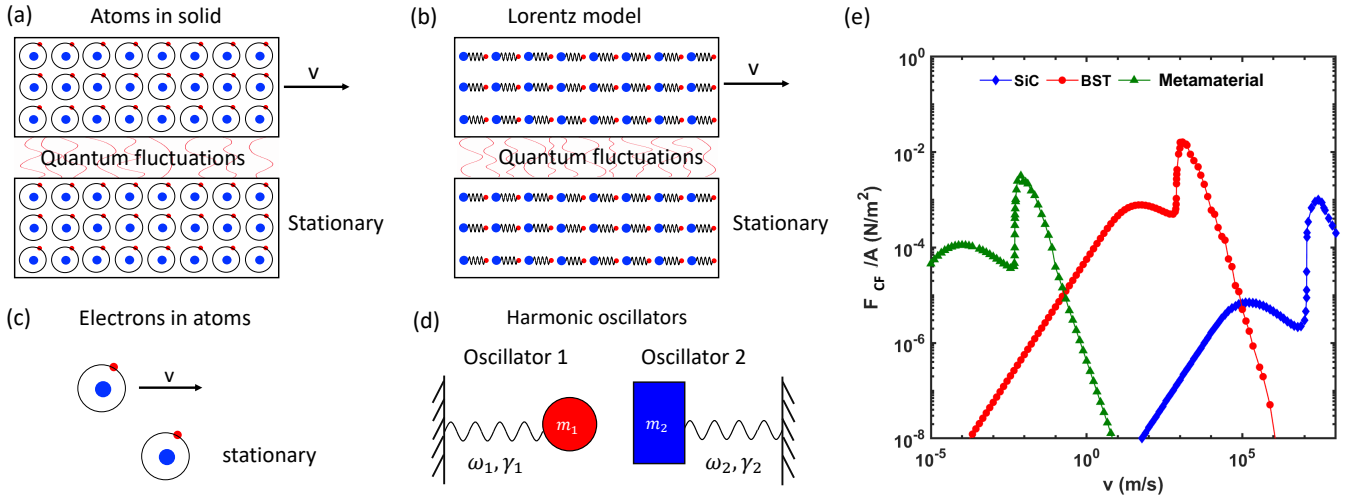


FIG. 1. **Casimir friction described by different models.** (a). When two closely spaced solid plates have a relative motion, they will experience the Casimir frictional force against the moving direction. The Casimir friction force essentially comes from the interaction between the incident photons and the electrons in solids. (b). The optical properties of solids can be modeled as Lorentz oscillators, which treat each discrete vibrational mode as a classical damped harmonic oscillator. The Casimir friction force here comes from the interaction between the incident photons and the phonons in solids. (c). In a microscopic point of view, the friction force exists between two moving atoms similar to the mechanism in Fig.(a). (d). In a microscopic point of view, the friction force exists between two classical damped oscillators with a relative motion, similar to the mechanism in Fig.(b). (e). Calculated Casimir frictional force between two moving dielectric materials at a separation of 100 nm. We notice that the resonant velocity are around 1×10^7 m/s, 1×10^3 m/s and 1×10^{-2} m/s for SiC, BST and a hypothetical metamaterial.

enhancement of Casimir friction coefficient F_{CF}/v by more than nine orders. Therefore, a metamaterial with a resonant frequency at kHz can significantly enhance the Casimir friction coefficient and makes the detection feasible. A normal relative motion also gives an enhancement of Casimir friction force compared to the parallel motion case [28].

Inspired by results in Fig.1(e), we develop a novel way to enhance the Casimir friction force at low relative velocities. When two solids have a relative motion, the quantum vacuum fluctuations between them induce the Casimir friction force (Fig.1(a)). This Casimir friction force essentially comes from the interaction between virtual photons, electrons and nuclei in the solids. The optical properties of macroscopic dielectric materials can be well modeled by Lorentz oscillators (Fig.1.(b)). Phonons (nuclear vibrations) play a critical role in the Casimir friction force at low velocities (Fig.1(e)). Casimir friction can also exist at a microscopic scale. Two moving atoms (Fig.1.(c)) will also experience Casimir friction due to quantum vacuum fluctuations, which has been calculated by modeling the two atoms as moving harmonic oscillators [11, 12, 36]. Similar to the two-atom system, a system consists of two moving mechanical oscillators will also experience the Casimir friction (Fig.1.(d)).

In this work, we measure the non-contact Casimir friction between two mechanical harmonic oscillators with relative motion as shown in Fig.1(d). The resonant frequencies of the mechanical resonators are about 5 kHz, similar to the metamaterial discussed above. This experimental

scheme significantly reduces the requirement of the relative moving velocity. For solids, the system energy is eventually dissipated by the electrical resistance and phonon damping in the solids. For mechanical harmonic oscillators, the system energy is dissipated by the mechanical loss of the resonators. We exploit a unique approach to minimize the non-dissipative Casimir force such that the frictional component can be isolated through a direct measurement. Besides, we can engineer the system loss to maximize the Casimir frictional force. This provides flexibility of tuning the Casimir frictional force. In this manuscript, we will show that we are able to increase a Casimir frictional force up to more than 3 pN at 0.38 mm/s. This is the first observation of Casimir frictional force. We show the linear velocity dependence of this dissipative Casimir friction force, revealing the dissipative nature of the frictional force. We also experimentally observed the quantum vacuum induced damping coefficient and isolated the instantaneous friction force.

Experimentally, our mechanical harmonic oscillators are two modified atomic force microscope (AFM) cantilevers which have nearly the same resonant frequencies to maximize the Casimir friction. A $70\text{-}\mu\text{m}$ -diameter microsphere is attached to the free end of one cantilever [37]. Both the microsphere and cantilever surfaces are coated with 100-nm-thick gold films. The gap between the microsphere and the flat surface of the other cantilever is on the order of 100 nm. They are coupled by the Casimir force [37–43] due to quantum vacuum fluctuations. More details of the dual-cantilever system can be

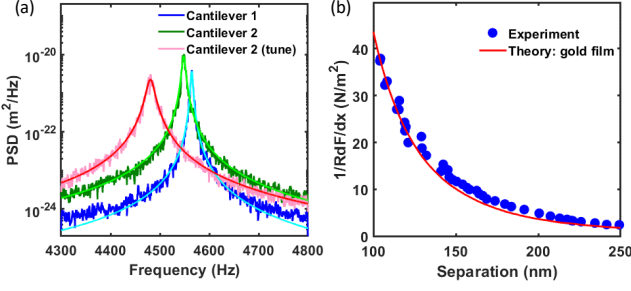


FIG. 2. **Measurement of Casimir interaction between two cantilevers.** (a). Power spectrum density (PSD) of cantilever 1 and cantilever 2. The blue one shows the PSD of cantilever 1 with a natural frequency of 4564.8 Hz. The green one shows the PSD of cantilever 2 with a natural frequency of 4548.9 Hz. In the Casimir force measurement, the frequency of cantilever 2 is shifted to 4481.5 Hz by PID control, in order to prevent resonant coupling, as shown in the red curve. (b). Measured Casimir force gradient is shown as a function of separation.

found in Supplementary Material Section I. The power spectrum density (PSD) of two cantilevers are shown in Fig.2.(a). The natural frequency of two cantilevers are $\omega_1 = 2\pi \times 4564.7$ Hz and $\omega_2 = 2\pi \times 4548.9$ Hz, respectively. The resonant frequency can be tuned by an external PID feedback. In order to measure the Casimir force without resonant coupling, the frequency of cantilever 2 is shifted to $\omega'_2 = 2\pi \times 4481.5$ Hz as shown in the red curve in Fig.2(a). We measure the Casimir force gradient $\frac{1}{R} \frac{dF}{dx}$ from the motion of cantilever 2 with the off-resonant frequency. The experimental results are shown in Fig.2.(b), which agree well with theoretical calculations (see Supplementary Material Section III) [44, 45]. Notice that the electrostatic force between two cantilevers due to surface patch potentials is cancelled out by applying additional voltages, similar to the method in [37]. Therefore, the coupling force between two cantilever is purely from Casimir interactions. Besides, the thermal contribution of the Casimir force is about 2% when the separation is less than 200 nm and when the system is at room temperature[37]. This unique dual-cantilever system has been used previously to demonstrate the Casimir effect as well as a Casimir diode[37]. However, the dissipative Casimir frictional force has not been measured before.

The measurement of the Casimir friction force is demonstrated as follows. The Casimir force between the two cantilevers is separation-dependent and sensitive to the motion of two cantilevers. Under the small vibration amplitude approximation, the Casimir force on cantilever 1 is written as $F_{Casimir} = F_{Casimir}(d) - \frac{dF_{Casimir}}{dx}(d)(x_1 + x_2)$. Here we focus on the coupling force on cantilever 1 which is $F_{couple} = -\frac{dF_{Casimir}}{dx}(d)x_2$. The Casimir coupling force between two cantilevers can be separated into the conservative term and the dissipative term as follows,

$$F_{couple} = F_{conservative} + F_{CF}, \quad (1)$$

where the dissipative force corresponds to the Casimir friction

force F_{CF} . Under a sinusoidal driving force on cantilever 1 with driving frequency ω_d , the two parts of the coupling force at the steady state are

$$F_{conservative} = \frac{(dF_{Casimir}/dx)^2}{m_2} \frac{\omega_2'^2 - \omega_d^2}{(\omega_2'^2 - \omega_d^2)^2 + \gamma_2^2 \omega_d^2} x_1, \\ F_{CF} = -\frac{(dF_{Casimir}/dx)^2}{m_2} \frac{\gamma_2}{(\omega_2'^2 - \omega_d^2)^2 + \gamma_2^2 \omega_d^2} \dot{x}_1, \quad (2)$$

where $\omega_1' = \omega_1 \sqrt{1 + \frac{1}{m_1 \omega_1^2} \frac{dF_{Casimir}}{dx}}$, $\omega_2' = \omega_2 \sqrt{1 + \frac{1}{m_2 \omega_2^2} \frac{dF_{Casimir}}{dx}}$ and they are the resonant frequency of two cantilevers in the presence of the Casimir force $F_{Casimir}$. $F_{conservative}$ is the conservative term which only depends on x_1 and F_{CF} is the dissipative term which only depends on \dot{x}_1 . More details about the derivation can be found in the Supplementary Material Section III. Here we consider a special case that when the driving frequency equals to the resonant frequency of cantilever 2 such that $\omega_d = \omega_2'$, the conservative force $F_{conservative}$ will be zero and the coupling force F_{couple} equals to the Casimir friction force F_{CF} . In this way, we can minimize the non-dissipative component of the coupling force and directly measure the Casimir friction.

In this experiment, we measure the instantaneous Casimir friction force and the results are shown in Fig.3. Here the damping rate of two cantilevers are tuned by the PID feedback loop to be $\gamma_1 = 2\pi \times 3.7$ Hz and $\gamma_2 = 2\pi \times 41.6$ Hz. The tuning details can be found in the Supplementary Material Section IV. Two cantilevers are closely spaced by a separation of 154 nm. Under a driving of 4521 Hz on cantilever 1, we record the instantaneous displacements and velocities of two cantilevers. Here the resonant frequency ω_2' of cantilever 2 at the presence of Casimir force is 4521 Hz. The time-dependent displacement x_1 and velocity v_1 of cantilever 1 are measured by the fiber interferometer and are shown in Fig.3.(a) and (b). Since the coupling force on cantilever 1 depends on the displacements of cantilever 2. We could measure x_2 and the force gradient $\frac{dF_{Casimir}}{dx}$ and get the instantaneous Casimir coupling force F_{couple} as shown in Fig.3.(c). The separation here is 154 nm. We notice that this Casimir coupling force is time varying, which eventually dissipates the energy by the mechanical loss of the cantilevers.

To further understand the distribution of conservative and dissipative terms in the coupling force, we show the recorded x_1 , x_2 and $-v_1/\omega_d$ in a short period of time in Fig.3.(d). When the driving frequency matches the resonant frequency of cantilever 2 such that $\omega_d = \omega_2'$, x_2 and $-v_1$ are in phase and the coupling force is linear with v_1 , revealing that it is a fully dissipative force and this is the Casimir friction force F_{CF} . This agrees with the conclusion in Eq.2. We can easily plot the relation between F_{couple} and v_1 in Fig.3.(e) for different velocities. In addition to the resonant driving of 4521 Hz (the driving frequency matches the resonant frequency of cantilever 2), we also present two off-resonant cases with a detuning of -10 Hz and -21 Hz. For the resonant case, F_{couple} and

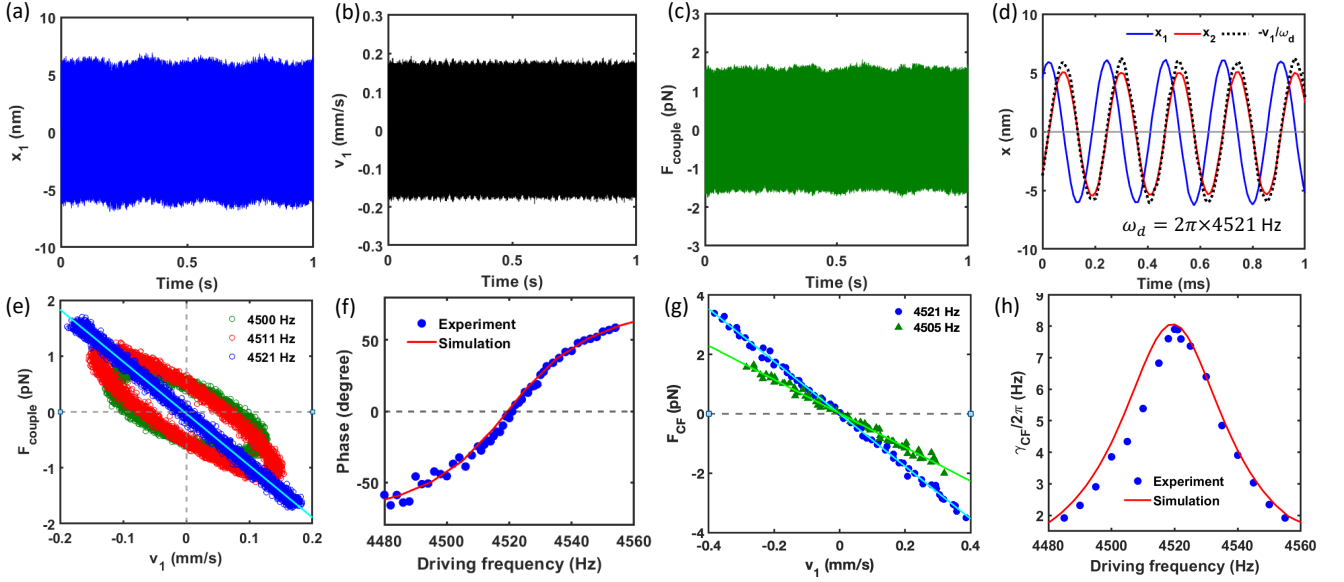


FIG. 3. **Measurement of Casimir friction force.** (a)-(c). Recorded x_1 , v_1 and $F_{couple} = \left| \frac{dF_{Casimir}}{dx} \right| x_2$ under the driving of 4521 Hz on cantilever 1 when the separation is 154 nm. Here the driving frequency matches the resonant frequency of cantilever 2. (d). v_1 and x_2 are in phase, revealing that the coupling force is fully dissipative. (e). The measured coupling force is shown for different driving frequencies and different velocities. When the driving frequency matches the resonant frequency of cantilever 2 such that $\omega_d = \omega'_2$, the coupling force F_{couple} is linear with the velocity v_1 and hence is a fully dissipative force. When the driving frequency has a detuning from resonance, the coupling force has a non-zero conservative component. (f). The relative phase between $-v_1$ and F_{couple} . It is noticed that for a resonant case, the phase becomes zero. (g). The Casimir friction force F_{CF} at each velocity is extracted from F_{couple} when x_1 equals to 0. (h). The Casimir friction damping rate $\gamma_{CF} = F_{CF}/m_1 v_1$ is shown for different driving frequency ω_d .

v_1 shows a linear relation because F_{couple} only comes from the dissipative force F_{CF} . For the off-resonant case, it shows an elliptical relation, depending on the detuning of the driving frequency. It indicates that the coupling force has a non-zero conservative component. The phase between $-v_1$ and F_{couple} is shown in Fig.3.(f). This is the first observation of Casimir friction and the heat dissipates as the mechanical loss of the resonators. Here two mechanical resonators have unique relative motion around their center-of-mass, which is different from the original vacuum friction problem with a constant relative velocity but has important similarities [3–6].

The key signature of the measured effect is that the Casimir friction force depends on the relative velocity. To understand the relation between the Casimir friction force and the velocity, we measure the friction force F_{CF} at different velocities by extracting the time-dependent v_1 and x_2 at a group of specific time when $x_1 = 0$. Under such condition, the conservative component of the coupling force in Eq.2 becomes zero so we can have $F_{couple} = F_{CF}$. The recorded F_{CF} is shown in Fig.3.(g). The measured Casimir friction force can reach up to more than 3 pN at a velocity around 4×10^{-4} m/s for a resonant case. A off-resonant driving will give a smaller friction force F_{CF} for the same velocity as shown in Fig.3.(g). A linear fitting gives the Casimir friction damping rate $\gamma_{CF} = F_{CF}/m_1 v_1$ for each driving frequency. We notice that, the measured Casimir friction damping rate can reach up to $2\pi \times 7.9$ Hz at a separation of 154 nm. Considering an

effective interaction area of $A = \frac{2}{3}\pi R d = 1.13 \times 10^{-11}$ m², we are able to detect a Casimir friction stress $\sigma_{CF} = F_{CF}/A = 0.3$ N/m² and a corresponding Casimir friction coefficient of $\Gamma_{CF} = F_{CF}/v_1 A = 783$ kgs⁻¹m⁻². A larger Casimir friction coefficient is expected to be realized at a smaller separation. This method significantly enhances the friction force and lowers the required velocity. As a comparison, the Casimir friction force coefficient between two moving SiC plates with a separation of 1 nm is calculated to be about 0.014 kgs⁻¹m⁻²[28]. Our experiment shows an enhancement of Casimir friction coefficient by several orders of magnitudes compared to the conventional scheme.

After measuring the Casimir friction force between two cantilevers, we measured the damping rate of cantilever 1 when two cantilevers are closely spaced. When cantilever 2 has a high mechanical loss γ_2 , cantilever 1 is expected to experience a large Casimir friction force and hence the damping rate γ_1 should increase. The measured γ_1 is shown in Fig.4.(a) and (b) for different γ_2 and separations. The damping rate is extracted by fitting the frequency response of cantilever 1 with a Lorentzian function. We notice that γ_1 increases as γ_2 increases and then saturated, eventually limited by the coupling strength between two cantilevers. The damping rate γ_1 can reach up to about $2\pi \times 12$ Hz at a separation of 99 nm. The separation dependence of γ_1 is shown in Fig.4.(b). In this case, the damping rate γ_1 of cantilever 1 reflects the energy loss by cantilever 1 mediated by quantum vacuum fluc-

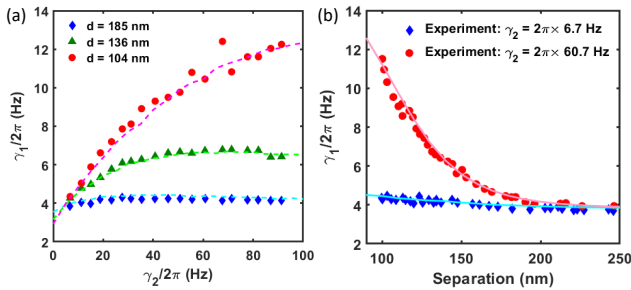


FIG. 4. **Measured mechanical loss through quantum vacuum fluctuations.** (a). The measured damping rate of cantilever 1 γ_1 is shown as a function of a tunable γ_2 . A higher mechanical loss γ_2 gives a larger γ_1 because of a stronger Casimir friction. The dashed curves correspond to the simulations. (b). The measured γ_1 is shown as a function of the separation.

tuations.

In conclusion, we have experimentally observed the Casimir friction force in a mechanical system. The mechanism of friction force essentially comes from an exchange of particles [6]. In our case, the Casimir friction comes from the exchange of virtual photons after interacting with the phonons in the mechanical system. The friction dissipates energy through the mechanical loss mediated by the Casimir force. Experimentally, we measure the instantaneous Casimir friction force up to more than 3 pN and demonstrate its linear dependence on velocity. To our best knowledge, this is the first measurement of Casimir friction force. Our detection of Casimir friction force will provide a better understanding of non-contact friction at the nanoscale [26, 27], and will be the precursor to observe the quantum vacuum friction under other conditions [11–21]. Since the non-contact friction applies to a lot of scenarios, our work will benefit the micro and nanomechanical technology as well as mechanical detection and sensors [24].

* teli@purdue.edu

- [1] D. Reiche, F. Intravaia, and K. Busch, Wading through the void: Exploring quantum friction and nonequilibrium fluctuations, *APL Photonics* **7**, 030902 (2022).
- [2] K. A. Milton, J. S. Høye, and I. Brevik, The reality of Casimir friction, *Symmetry* **8**, 29 (2016).
- [3] E. V. Teodorovich, On the contribution of macroscopic van der waals interactions to frictional force, *Proceedings of the Royal Society of London. Series A, Mathematical and Physical Sciences* **362**, 71 (1978).
- [4] W. L. Schaich and J. Harris, Dynamic corrections to van der waals potentials, *Journal of Physics F: Metal Physics* **11**, 65 (1981).
- [5] L. S. Levitov, Van der waals' friction, *Europhysics Letters (EPL)* **8**, 499 (1989).
- [6] J. B. Pendry, Shearing the vacuum - quantum friction, *Journal of Physics: Condensed Matter* **9**, 10301 (1997).
- [7] D. Oue, K. Ding, and J. Pendry, Noncontact frictional force between surfaces by peristaltic permittivity modulation, *Physical Review A* **107**, 063501 (2023).
- [8] T. G. Philbin and U. Leonhardt, No quantum friction between uniformly moving plates, *New Journal of Physics* **11**, 033035 (2009).
- [9] J. B. Pendry, Quantum friction—fact or fiction?, *New Journal of Physics* **12**, 033028 (2010).
- [10] A. I. Volokitin and B. N. J. Persson, Comment on ‘no quantum friction between uniformly moving plates’, *New Journal of Physics* **13**, 068001 (2011).
- [11] J. S. Høye and I. Brevik, Casimir friction force and energy dissipation for moving harmonic oscillators, *EPL (Europhysics Letters)* **91**, 60003 (2010).
- [12] J. S. Høye and I. Brevik, Casimir friction in terms of moving harmonic oscillators: equivalence between two different formulations, *The European Physical Journal D* **64**, 1 (2011).
- [13] L. Ge, Negative vacuum friction in terahertz gain systems, *Physical Review B* **108**, 045406 (2023).
- [14] A. Fernández and C. D. Fosco, Spatial dependence of Casimir friction in graphene, *Physical Review D* **108**, 116010 (2023).
- [15] X. Guo, K. A. Milton, G. Kennedy, and N. Pourtolami, Quantum friction in the presence of a perfectly conducting plate, *Physical Review A* **107**, 062812 (2023).
- [16] A. I. Volokitin and B. N. J. Persson, Quantum friction, *Phys. Rev. Lett.* **106**, 094502 (2011).
- [17] R. Zhao, A. Manjavacas, F. J. García de Abajo, and J. B. Pendry, Rotational quantum friction, *Phys. Rev. Lett.* **109**, 123604 (2012).
- [18] F. Intravaia, M. Oelschläger, D. Reiche, D. A. R. Dalvit, and K. Busch, Quantum rolling friction, *Phys. Rev. Lett.* **123**, 120401 (2019).
- [19] J. Ahn, Z. Xu, J. Bang, P. Ju, X. Gao, and T. Li, Ultrasensitive torque detection with an optically levitated nanorotor, *Nature Nanotechnology* **15**, 89 (2020).
- [20] P. Ju, Y. Jin, K. Shen, Y. Duan, Z. Xu, X. Gao, X. Ni, and T. Li, Near-field ghz rotation and sensing with an optically levitated nanodumbbell, *Nano letters* **23**, 10157 (2023).
- [21] M. B. Farías, F. C. Lombardo, A. Soba, P. I. Villar, and R. S. Decca, Towards detecting traces of non-contact quantum friction in the corrections of the accumulated geometric phase, *npj Quantum Information* **6**, 25 (2020).
- [22] I. Dorofeyev, H. Fuchs, G. Wenning, and B. Gotsmann, Brownian motion of microscopic solids under the action of fluctuating electromagnetic fields, *Phys. Rev. Lett.* **83**, 2402 (1999).
- [23] B. Gotsmann and H. Fuchs, Dynamic force spectroscopy of conservative and dissipative forces in an al-au(111) tip-sample system, *Phys. Rev. Lett.* **86**, 2597 (2001).
- [24] B. Gotsmann, Sliding on vacuum, *Nature Materials* **10**, 87 (2011).
- [25] M. Oelschläger, D. Reiche, C. H. Egerland, K. Busch, and F. Intravaia, Electromagnetic viscosity in complex structured environments: From blackbody to quantum friction, *Phys. Rev. A* **106**, 052205 (2022).
- [26] Y. Mo, K. T. Turner, and I. Szlufarska, Friction laws at the nanoscale, *Nature* **457**, 1116 (2009).
- [27] N. Kavokine, M.-L. Bocquet, and L. Bocquet, Fluctuation-induced quantum friction in nanoscale water flows, *Nature* **602**, 84 (2022).
- [28] A. I. Volokitin and B. N. J. Persson, Resonant photon tunneling enhancement of the van der waals friction, *Phys. Rev. Lett.* **91**, 106101 (2003).
- [29] Y. Guo and Z. Jacob, Singular evanescent wave resonances in moving media, *Opt. Express* **22**, 26193 (2014).
- [30] Y. Guo and Z. Jacob, Giant non-equilibrium vacuum friction:

- role of singular evanescent wave resonances in moving media, *Journal of Optics* **16**, 114023 (2014).
- [31] Z. Xu, Z. Jacob, and T. Li, Enhancement of rotational vacuum friction by surface photon tunneling, *Nanophotonics* **10**, 537 (2021).
- [32] A. Volokitin, Resonant photon emission during relative sliding of two dielectric plates, *Modern Physics Letters A* **35**, 2040011 (2020).
- [33] F. Khosravi, W. Sun, C. Khandekar, T. Li, and Z. Jacob, Giant enhancement of vacuum friction in spinning YIG nanospheres, arXiv preprint arXiv:2401.09563 10.48550/arXiv.2401.09563 (2024).
- [34] A. Manjavacas, F. J. Rodríguez-Fortuño, F. J. García de Abajo, and A. V. Zayats, Lateral Casimir force on a rotating particle near a planar surface, *Phys. Rev. Lett.* **118**, 133605 (2017).
- [35] A. I. Volokitin and B. N. J. Persson, Theory of friction: the contribution from a fluctuating electromagnetic field, *Journal of Physics: Condensed Matter* **11**, 345 (1999).
- [36] J. S. HØYE and I. BREVIK, Casimir friction force for moving harmonic oscillators, *International Journal of Modern Physics A* **27**, 1260011 (2012).
- [37] Z. Xu, X. Gao, J. Bang, Z. Jacob, and T. Li, Non-reciprocal energy transfer through the casimir effect, *Nature nanotechnology* **17**, 148 (2022).
- [38] H. B. G. Casimir and D. Polder, The influence of retardation on the london-van der waals forces, *Phys. Rev.* **73**, 360 (1948).
- [39] S. K. Lamoreaux, Demonstration of the casimir force in the 0.6 to 6 μ m range, *Physical Review Letters* **78**, 5 (1997).
- [40] Z. Xu, P. Ju, X. Gao, K. Shen, Z. Jacob, and T. Li, Observation and control of casimir effects in a sphere-plate-sphere system, *Nature Communications* **13**, 6148 (2022).
- [41] R. Zhao, L. Li, S. Yang, W. Bao, Y. Xia, P. Ashby, Y. Wang, and X. Zhang, Stable casimir equilibria and quantum trapping, *Science* **364**, 984 (2019).
- [42] B. Munkhbat, A. Canales, B. Küçüköz, D. G. Baranov, and T. O. Shegai, Tunable self-assembled casimir microcavities and polaritons, *Nature* **597**, 214 (2021).
- [43] J. M. Pate, M. Goryachev, R. Y. Chiao, J. E. Sharping, and M. E. Tobar, Casimir spring and dilution in macroscopic cavity optomechanics, *Nature Physics* **16**, 1117 (2020).
- [44] E. M. Lifshitz, The theory of molecular attractive forces between solids, *Sov. Phys. JETP* **2**, 73 (1956).
- [45] J. Błocki, J. Randrup, W. J. Świątecki, and C. F. Tsang, Proximity forces, *Annals of Physics* **105**, 427 (1977).

SUPPLEMENTARY MATERIAL

Experimental setup and force measurement

The Casimir friction measurement system consists of two modified atomic force microscope (AFM) cantilevers as shown in Fig.5, similar to the setup in [37]. The left cantilever has a dimension of $450 \mu\text{m} \times 50 \mu\text{m} \times 2 \mu\text{m}$. A $70\text{-}\mu\text{m}$ -diameter polystyrene sphere is attached to the free end of the left cantilever. The right cantilever has a dimension of $500 \mu\text{m} \times 100 \mu\text{m} \times 1 \mu\text{m}$. Additional 100-nm-thick gold layers are coated on both the sphere and cantilever surfaces to ensure good conductivity. Two piezo chips are mounted at the end of the cantilevers to control the motion. In the Casimir friction measurement, two fiber interferometers with a 1310-nm-wavelength laser are implemented to measure the instantaneous motion and velocity of two cantilevers. Besides, a PID feedback control loop is applied to cantilever 2 through the piezo chips to tune its damping rate and resonant frequency. More details of the tunable damping rate can be found in section .

Calculation of Casimir friction between two sliding plates

We consider two perfectly smooth plates moving with a relative parallel motion. The schematic is shown in Fig.6. In the nonrelativistic limit ($v \ll c$) and near-field limit ($d \ll c\hbar/k_B T$), the Casimir friction force per unit area experienced by the plates is [35]

$$F_{CF} = \frac{\hbar}{4\pi^3} \int_{-\infty}^{\infty} dq_x \int_{-\infty}^{\infty} dq_y \int_0^{\infty} d\omega q_x \left\{ \frac{\text{Im}(R_{1p}(\omega)) \text{Im}(R_{2p}(\omega - q_x v)) e^{-2qd}}{|1 - e^{-2qd} R_{1p}(\omega) R_{2p}(\omega - q_x v)|^2} + (p \leftrightarrow s) \right\} \times [n_2(\omega - q_x v) - n_1(\omega)] + (1 \leftrightarrow 2), \quad (3)$$

where v is the relative velocity between two plates, $n_{1,2}(\omega) = \frac{1}{\exp(\hbar\omega/k_B T_j) - 1}$ is the Bose–Einstein distribution function at temperature T_j and $j = 1, 2$ are for two different plates. $R_{jp(s)}$ is the reflection amplitude of plate j for p and s polarized electromagnetic waves and it is written as

$$R_{jp} = \frac{\epsilon_j p - s_j}{\epsilon_j p + s_j}, \quad R_{js} = \frac{\epsilon_j - s_j}{\epsilon_j + s_j}. \\ q = \sqrt{q_x^2 + q_y^2}, \quad p = \sqrt{\frac{\omega^2}{c^2} - q^2}, \quad s_j = \sqrt{\frac{\omega^2}{c^2} \epsilon_j - q^2}. \quad (4)$$

Here we calculate the Casimir friction force between two sliding plates at a separation of 100 nm. The temperature of both plates are at 300 K. The calculated friction force is shown in Fig.1.(e) in the main text. The dielectric functions of different

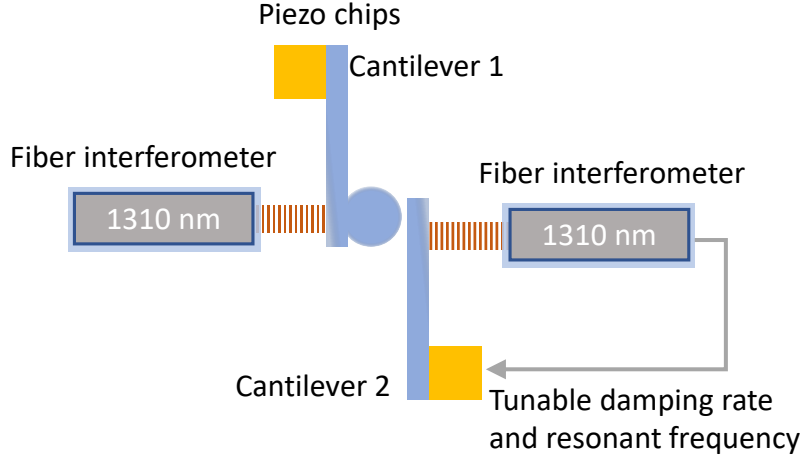


FIG. 5. The schematic of the Casimir friction measurement setup. Two modified AFM cantilevers are used to detect the dissipative Casimir friction force. Two fiber interferometers are implemented to measure the motions of the two cantilevers. The piezo chips at the end of the cantilevers are used to control the motion of the cantilevers. A PID feedback control loop is applied to cantilever 2 through the piezo chips to tune its damping rate and resonant frequency.

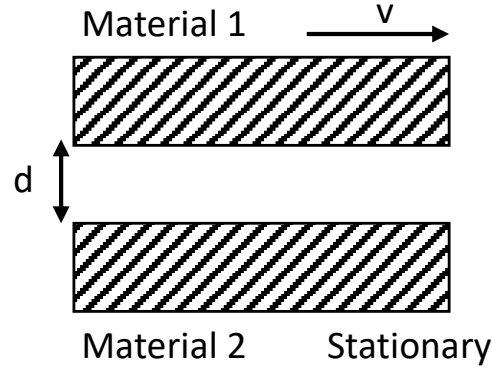


FIG. 6. Two perfectly smooth and infinitely thick plates are separated by a distance d and they are having a relative motion with a velocity v . They experience a friction force against the moving direction because of the quantum vacuum fluctuations.

dielectric materials can be modeled as Lorentz oscillators, which treat each discrete vibrational mode as a classical damped harmonic oscillator. The dielectric functions can be written as

$$\epsilon(\omega) = \epsilon_{\infty} \left(1 + \frac{\omega_L^2 - \omega_T^2}{\omega_T^2 - \omega^2 - i\gamma\omega} \right). \quad (5)$$

The parameters for SiC are $\epsilon = 6.7$, $\omega_L = 1.8 \times 10^{14} \text{ s}^{-1}$, $\omega_T = 1.5 \times 10^{14} \text{ s}^{-1}$ and $\gamma = 8.9 \times 10^{11} \text{ s}^{-1}$ [34]. The parameters for barium barium strontium titanate (BST) are $\epsilon_{\infty} = 2.9$, $\omega_L = 1.3 \times 10^{10} \text{ s}^{-1}$, $\omega_T = 5.7 \times 10^9 \text{ s}^{-1}$ and $\gamma = 2.8 \times 10^8 \text{ s}^{-1}$ [31]. The real and imaginary part of the dielectric function for these two materials are shown in Fig.7.(a) and (b). In addition, we investigate a hypothetical metamaterial that has a resonant frequency at 5 kHz and a dielectric function that can be described by the Lorentz model:

$$\epsilon(\omega) = \epsilon_{\infty} \left(1 + \frac{B}{\omega_T^2 - \omega^2 - i\gamma\omega} \right), \quad (6)$$

where the parameters are engineered to be $\omega_T = 2\pi \times 5000 \text{ s}^{-1}$, $\gamma = 2\pi \times 100 \text{ s}^{-1}$, $B = 5 \times 10^9 \text{ s}^{-2}$.

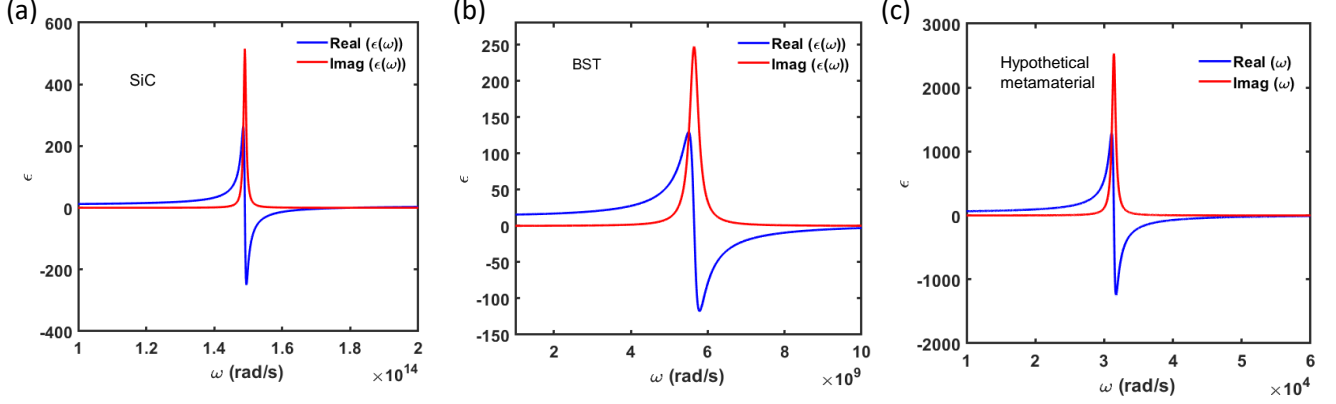


FIG. 7. The dielectric function for three different materials.

Casimir friction force between two harmonic oscillators

In this part, we will show the equations of motion in details and derive the dissipative Casimir friction force. The equation of motion of the two-cantilever system can be written as

$$\begin{aligned} m_1 \ddot{x}_1 + m_1 \gamma_1 \dot{x}_1 + m_1 \omega_1^2 x_1 &= F_{Casimir}(t) + F_d(t), \\ m_2 \ddot{x}_2 + m_2 \gamma_2 \dot{x}_2 + m_2 \omega_2^2 x_2 &= F_{Casimir}(t), \end{aligned} \quad (7)$$

where the driving force is $F_d = F_0 \cos(\omega_d t)$ with driving amplitude F_0 and driving frequency ω_d . The Casimir force here under the proximity-force approximation (PFA)[45] is given by

$$F_{Casimir}(x, T) = -2\pi R E(x, T), \quad (8)$$

where $E(x, T)$ is the Casimir pressure between two infinitely thick plates. At a finite temperature and at a separation x , the Casimir pressure $E(x, T)$ is[44]

$$E(x, T) = \frac{k_B T}{2\pi} \sum_{l=0}^{\infty} \int_0^{\infty} k_{\perp} dk_{\perp} \{ \ln[1 - r_{TM}^2(i\xi_l, k_{\perp})e^{-2xq}] + \ln[1 - r_{TE}^2(i\xi_l, k_{\perp})e^{-2xq}] \} \quad (9)$$

where $\xi_l = \frac{2\pi k_B T l}{\hbar}$ is the Matsubara frequency and the prime on the summation indicates that the $l = 0$ term will be multiplied by $1/2$. We notice that the Casimir force is separation-dependent and very sensitive to the oscillation of two cantilevers so the time-dependent Casimir force is written as $F_{Casimir}(t) = F_{Casimir}(d - x_1(t) - x_2(t))$. When the oscillation of two cantilevers near the equilibrium are far smaller than the separation, the Casimir force can be expanded to the first order and be written as

$$F_{Casimir}(d - x_1 - x_2) = F_{Casimir}(d) - \frac{dF_{Casimir}}{dx}(d)(x_1 + x_2). \quad (10)$$

Therefore, the equations of motion will become

$$\begin{aligned} m_1 \ddot{x}_1 + m_1 \gamma_1 \dot{x}_1 + m_1 \omega_1'^2 x_1 &= J x_2 + F_0 \cos(\omega_d t), \\ m_2 \ddot{x}_2 + m_2 \gamma_2 \dot{x}_2 + m_2 \omega_2'^2 x_2 &= J x_1. \end{aligned} \quad (11)$$

where $\omega_1' = \omega_1 \sqrt{1 + \frac{1}{k_1} \frac{dF_{Casimir}}{dx}}$, $\omega_2' = \omega_2 \sqrt{1 + \frac{1}{k_2} \frac{dF_{Casimir}}{dx}}$ and $J = -\frac{dF_{Casimir}}{dx}(d)$. J is a positive value since the Casimir force in our vacuum system is an attractive interaction. Here we focus on the coupling force on cantilever 1 which is $F_{couple} = J x_2$. The general solutions for the above equations are

$$\begin{aligned} x_1 &= \frac{(\omega_2'^2 - \omega_d^2 + i\gamma_2 \omega_d) f}{(\omega_1'^2 - \omega_d^2 + i\gamma_1 \omega_d)(\omega_2'^2 - \omega_d^2 + i\gamma_2 \omega_d) - j^2} \times \exp(i\omega_d t), \\ x_2 &= \sqrt{\frac{m_1}{m_2}} \frac{j f}{(\omega_1'^2 - \omega_d^2 + i\gamma_1 \omega_d)(\omega_2'^2 - \omega_d^2 + i\gamma_2 \omega_d) - j^2} \times \exp(i\omega_d t), \end{aligned} \quad (12)$$

where we have $j = J/\sqrt{m_1 m_2}$ and $f = F/m_1$. When the driving frequency matches the resonant frequency of cantilever 2 such that $\omega_d = \omega'_2$, the solutions will become

$$\begin{aligned} x_1 &= \frac{i\gamma_2 \omega'_2 f}{(\omega_1'^2 - \omega_2'^2 + i\gamma_1 \omega'_2) i\gamma_2 \omega'_2 - j^2} \exp(i\omega'_2 t), \\ x_2 &= \sqrt{\frac{m_1}{m_2}} \frac{jf}{(\omega_1'^2 - \omega_2'^2 + i\gamma_1 \omega'_2) i\gamma_2 \omega'_2 - j^2} \exp(i\omega'_2 t). \end{aligned} \quad (13)$$

Under such case, the relation between x_1 and x_2 will be

$$x_2 = -i \sqrt{\frac{m_1}{m_2}} \frac{j}{\gamma_2 \omega'_2} x_1 = -\frac{J}{m_2 \gamma_2 \omega_2'^2} \dot{x}_1, \quad (14)$$

which means that we can rewrite the coupling term on cantilever 1 such that

$$F_{couple} = Jx_2 = -\frac{J^2}{m_2 \gamma_2 \omega_d^2} \dot{x}_1. \quad (15)$$

Therefore, for a special driving that $\omega_d = \omega'_2$, the coupling force all comes from the dissipative Casimir friction force. There is no conservative part under such condition. A more general case of the coupling force, the conservative force and the dissipative friction force will be

$$\begin{aligned} F_{couple} &= \frac{J^2}{m_2} \left(\frac{\omega_2'^2 - \omega_d^2}{(\omega_2'^2 - \omega_d^2)^2 + \gamma_2^2 \omega_d^2} x_1 - \frac{\gamma_2}{(\omega_2'^2 - \omega_d^2)^2 + \gamma_2^2 \omega_d^2} \dot{x}_1 \right), \\ F_{conservative} &= \frac{J^2}{m_2} \frac{\omega_2'^2 - \omega_d^2}{(\omega_2'^2 - \omega_d^2)^2 + \gamma_2^2 \omega_d^2} x_1, \\ F_{CF} &= -\frac{J^2}{m_2} \frac{\gamma_2}{(\omega_2'^2 - \omega_d^2)^2 + \gamma_2^2 \omega_d^2} \dot{x}_1, \end{aligned} \quad (16)$$

where the conservative part $F_{conservative}$ only depends on x_1 and the dissipative part F_{CF} only depends on \dot{x}_1 . The main idea of this paper is to measure the dissipative Casimir friction force F_{CF} mediated by the quantum vacuum fluctuations and its dependence of the mechanical intrinsic loss of the system.

Calibration of the tunable damping rate of the harmonic resonators

In the experiment, we monitor the oscillation of two cantilevers by the fiber interferometers at each side. A PID feedback control loop is applied to cantilever 2 through the piezo chips to control the damping rate of cantilever 2 as shown in Fig.5. We use the sweeper function in Zurich Instruments MFLI device to calibrate the damping rate of two cantilevers. The frequency response of a cantilever is fitted with the Lorentzian function to extract the damping rate. An example of the frequency response recorded by the sweeper function is shown in Fig.8.(a) and this corresponds to two special case of $D = 0$ and $D = -8u$, where D is the derivative parameters in the PID control. From the Lorentzian fitting, we can get that $D = 0$ indicates a natural damping rate of $\gamma_2 = 2\pi \times 6.7$ Hz and $D = -8u$ gives a damping rate of $\gamma_2 = 2\pi \times 41.6$ Hz. The calibrated damping rate and resonant frequency at different derivative parameters D is shown in Fig.8.(b) and (c). Experimentally, we can tune the damping rate of cantilever 2 up to $2\pi \times 91$ Hz.

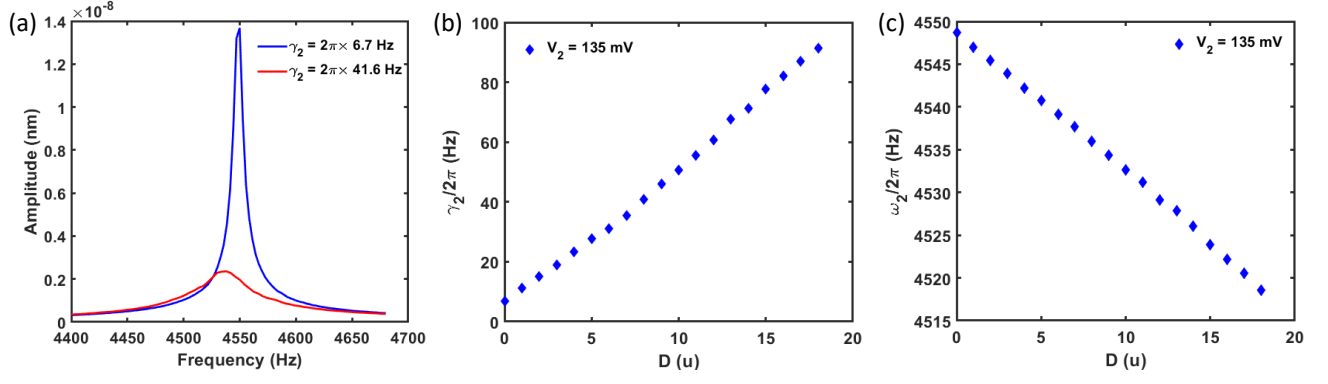


FIG. 8. Damping rate calibrated from the frequency response. (a). An example of the frequency response of cantilever 2 for two PID cases that $D = 0$ and $D = -8u$, which correspond to $\gamma_2 = 2\pi \times 6.7$ Hz and $\gamma_2 = 2\pi \times 41.6$ Hz. (b). The calibrated damping rate γ_2 is shown as a function of the externally controlled derivative parameters D . (c). The calibrated resonant frequency is shown as a function of the controlled derivative parameters D .